J Biol Inorg Chem (2004) 9: 423–428
DOI 10.1007/s00775-004-0542-3

ORIGINAL ARTICLE

**Il Yeong Park · Buhyun Youn · Jill L. Harley
Marly K. Eidsness · Eugene Smith · Toshiko Ichiye
ChulHee Kang**

The unique hydrogen bonded water in the reduced form of *Clostridium pasteurianum* rubredoxin and its possible role in electron transfer

Received: 20 January 2004 / Accepted: 15 March 2004 / Published online: 6 April 2004

Abstract Rubredoxin is a small iron-sulfur (FeS_4) protein involved in oxidation–reduction reactions. The side chain of Leu41 near the iron-sulfur center has two conformations, which we suggested previously serve as a gate for a water molecule during the electron transfer process. To establish the role of residue 41 in electron transfer, an [L41A] mutant of *Clostridium pasteurianum* rubredoxin was constructed and crystallized in both oxidation states. Despite the lack of the gating side chain in this protein, the structure of the reduced [L41A] rubredoxin reveals a specific water molecule in the same position as observed in the reduced wild-type rubredoxin. In contrast, both the wild-type and [L41A] rubredoxins in the oxidized state do not have water molecules in this location. The reduction potential of the [L41A] variant was ~50 mV more positive than wild-type. Based on these observations, it is proposed that the site around the Sγ of Cys9 serves as a port for an electron acceptor. Lastly, the Fe–S distances of the reduced rubredoxin are expanded, while the hydrogen bonds between Sγ of the cysteines and the backbone amide nitrogens are shortened compared to its oxidized counterpart. This small structural perturbation in the Fe(II)/Fe(III) transition is closely related to the small energy difference which is important in an effective electron transfer agent.

Keywords Crystal structure · Electron transfer · L41A mutant · Redox protein · Rubredoxin

I. Y. Park · B. Youn · C. Kang (✉)
School of Molecular Biosciences,
Washington State University,
Pullman, WA 99164-4660, USA
E-mail: chkang@wsunix.wsu.edu
Tel.: +1-509-3351409
Fax: +1-509-3359688

I. Y. Park
College of Pharmacy,
Chungbuk National University,
361-763 Cheongju, Korea

J. L. Harley · M. K. Eidsness
Department of Chemistry,
University of Georgia, Athens,
GA 30602-2556, USA

E. Smith
Wilkes Honors College,
Jupiter, FL 33458, USA

T. Ichiye
Department of Chemistry,
Georgetown University,
Washington,
DC 20057-1227, USA

Introduction

Oxidation–reduction is essential in bioenergetics or scavenging processes of life. Not only does it provide the means for transforming solar and chemical energy into an utilizable form for all living organisms, it also extends into a range of metabolic processes. The sign and relative magnitude of the reduction potential is a determining factor for transferring electrons from one component to another. In biological processes, such as photosynthesis, respiration, and nitrogen fixation, electron transfer proteins determine the rate and the direction of the electron transfer reaction by modulating the reduction potential of their redox sites.

To date, however, the basic mechanisms of establishing and controlling the reduction potential of electron transfer proteins are largely unknown. Homologous redox proteins with the same redox sites have differences in reduction potentials that span a few hundred millivolts [1, 2]. The structural basis leading to the differences in reduction potential is crucial to understanding how the electron transfer protein can function. A single point mutation can drastically modify the reduction potential and subsequently influence the electron transfer rate. Despite the rapidly growing number of known rubredoxins with different reduction potentials and structural information, the factors that contribute to differences in reduction potential are

complex and quantitative predictions are still not possible. For example, factors such as subtle shifts in the local environment and solvent accessibility may be redox state dependent and dynamic. This complexity has made it impossible to determine basic mechanisms simply by examining a crystal structure of a single representative native protein in one oxidation state. In fact, examining single structures has often led to very contradictory interpretations of the physical origins of reduction potential differences. To understand differences in reduction potential, it is clearly necessary to have highly accurate structures of both native and mutant proteins in both the oxidized and reduced states.

Efforts have been made to understand the determining factors for the reduction potential using rubredoxin as a model system [3, 4, 5, 6]. It is a small redox protein with a single iron atom redox site tetrahedrally coordinated by four cysteinyl thiolates. The reduction potentials of rubredoxins (Rds) cover the range from −100 to +60 mV [7]. Unlike heme proteins, the redox sites of Rds are all relatively small so that the area of direct interaction with the protein is much smaller.

Two cysteines (Cys6 and Cys39) are located inside the molecule, while the other two cysteines (Cys9 and Cys42) are somewhat solvent accessible. The Sγ atom of Cys42 is partially covered by the side chains of two hydrophobic residues of Val8 and Val44, and the Sγ of Cys9 is also partially covered by the side chain of Leu41. Unlike the close van der Waals contact between Val8 and Val44 over Cys42, Leu41 has freedom of movement in its side chain without perturbing the backbone or overall structure of the protein. A rigid backbone for this solvent-exposed residue is provided by its neighbors: Pro40, Cys 39, and Cys42. The crystal structures of Rds deposited in the Protein Data Bank show the side chain of residue 41 in two conformations (1B2O, 1C09, 1FHH, 1FHM, 1IRO, 4RXN; Fig. 1) [8].

High-resolution crystal structures of both oxidation states of *Clostridium pasteurianum* (Cp) Rd were previously determined to elucidate their structural differences. A string of water molecules hydrogen-bonded to Sγ of Cys9 was only observed in its reduced state, and it was suggested that Leu41 near the iron-sulfur center serves as a gate for water entry during the redox reaction [5, 9, 10].

To test the role of the side chain of this Leu41 as a "flip-flop" gate, a variant of Leu41Ala (L41A) of *C. pasteurianum* rubredoxin was constructed and crystallized. In addition to oxidized crystals, two kinds of reduced crystals were produced: one was obtained from crystallization of the reduced protein solution under a nitrogen environment; the other was formed via direct reduction of the oxidized red crystal to the transparent colorless one with sodium dithionite.

Materials and methods

Cloning, over-expression, and purification of L41A Cp Rd variant

The [L41A] Cp Rd clone was constructed by site-directed mutagenesis of the Cp Rd gene in plasmid pT7-7 [11] by the QuickChange procedure (Stratagene, La Jolla, Calif.), using complementary primers to introduce the Ala codon, 5′-TGG GTT TGC CCG GCC TGC GGT GTT GG-3′ and 5′-CCA ACA CCG CAG GCC GGG CAA ACC CA-3′. The QuickChange product was transformed into *Escherichia coli* strain XL-1 Blue (Stratagene) according to the manufacturer's instructions. A few single colonies grew on Luria-Bertani (LB) medium and 1.5% agar (Difco Bacto) in the presence of ampicillin (100 μg/mL). One colony was selected and amplified by standard procedures [11] in a 100-mL growth and the plasmid purified by a QIAGEN midi-prep (QIAGEN, Valencia, Calif.). The plasmid sequence was determined by Sequetech (Mountain View, Calif.) from the T7 primer site upstream of the Rd gene start. The L41A codon change was confirmed, as well as the integrity of the remaining bases of the Cp Rd gene,

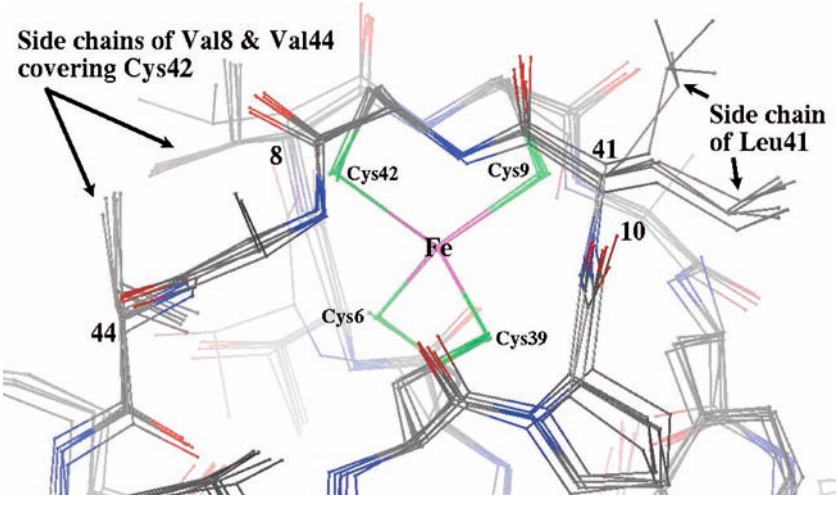

Fig. 1 The redox center of rubredoxin and the conformational variation of the side chain of Leu41 (six structures overlapped: 1B20, 1C09, 1FHH, 1FHM, 1IRO, 4RXN). The Sγ of Cys42 is covered by the close van der Waals contact between Val8 and Val44

and the plasmid was named pL41A Cp Rd. It was then transformed into the *E. coli* expression strain, BL-21 Gold (DE3) (Stratagene). Cultures were grown at 250 rpm at 37 °C in 4 L of LB medium supplemented with ampicillin (100 μg/mL) and induced by the addition of IPTG (0.4 mM final concentration); growth continued for 5 h, then the cells were harvested by centrifugation at 6000×*g*, and lysed following published procedures [12].

[L41A] Cp Rd over-expressed protein was separated from other *E. coli* proteins by passage over a Hi-Trap Q 5-mL column (Amersham Biosciences) on an ÅKTA FPLC system (Amersham Biosciences). The red-colored [L41A] Cp Rd protein eluted at around 50% B in a 20-column-volume gradient from 0 to 100% B, where buffer A is 50 mM Tris-HCl, pH 7.6, and buffer B is buffer A + 1.0 M NaCl. Fractions containing a red color were pooled, diluted with buffer A to reduce the NaCl concentration, loaded onto a Resource Q 6-mL column (Amersham Biosciences), and eluted under the same conditions as described above. A final round of purification was performed on a MonoQ HR10/10 column (Amersham Biosciences) under the same conditions. [L41A] Cp Rd protein was concentrated in YM3 Centricons (Millipore) to about 5 mM, based on the visible absorbance extinction coefficient of the 490 nm peak [12].

Electrochemical measurements

Cyclic voltammetry measurements were recorded via a BAS CV 50 W potentiostat (Bioanalytical Systems, Lafayette, Ind.). Experiments were carried out at room temperature using a microscale electrochemical cell as previously described [13], with a pyrolytic graphite working electrode, a platinum counter electrode, and a saturated Ag/AgCl reference electrode. All potentials are reported versus the standard hydrogen electrode.

Crystallization of oxidized and reduced forms of Cp Rd variant L41A

The oxidized crystals of [L41A] Cp Rd were produced by vapor diffusion against 2.3 M ammonium sulfate, 0.1 M sodium acetate at pH 4.0, and 10 mM sodium chloride (oxidized). The reduced crystals were produced against 2.3 M ammonium sulfate and 0.1 M sodium acetate at pH 4.6, with 10 mM sodium dithionite as the reducing agent under a nitrogen environment (drop-reduced). Each of 2 μL of the protein solution was mixed with 2 μL of the reservoir solutions and placed over the reservoir as a hanging drop. The deep-red colored crystals of the oxidized form, and the transparent, colorless crystals of the reduced form, were grown to a suitable size for crystallographic study within 4 days. Another kind of reduced crystal was also produced by dipping the oxidized crystal into a cryo-solution containing sodium dithionite just before mounting on the goniometer head (soaked). The colorless (reduced) state did not change throughout the data collection procedure.

Data collection, molecular replacement, and crystallographic refinement

All data for the three kinds of crystals (oxidized, drop-reduced, and soaked) of [L41A] Cp Rd were collected at the Advanced Light Source at Berkeley (beam line 8.2.1, ADSC Q210 CCD) under a −160 °C nitrogen stream with a crystal-to-detector distance of 110 mm (X-ray wavelength 1.0332 Å). All three crystals belong to the same space group of *R*3 in the trigonal crystal system. The crystal data are listed in Table 1, together with the refinement statistics.

The structures of all three Cp Rds were solved by molecular replacement methods using atomic coordinates of the previously solved oxidized Cp Rd (1FHH). The initial coordinates were obtained by the AMoRe software package [14]. The rigid-body refinement of the initial position was carried out using 15.0 Å to 3.0 Å resolution data and produced *R*-values around 30%. Then the structures were refined by X-PLOR [15]. After several cycles of positional refinement and temperature factor refinement, we were able to fit all of the residues to the electron density. The solvent molecules were identified in difference Fourier maps, and after several cycles of refinements the peaks with diffused density ($B > 40.0$) were discarded. One sulfate ion was found

Table 1 Summary of data collection and refinement statistics

	Oxidized	Red (drop)	Red (soak)
Space group	*R*3	*R*3	*R*3
Cell constants			
$a = b$(Å)	62.79	63.07	63.04
c (Å)	32.80	32.60	32.69
Molecule in an asymmetric unit	1	1	1
Resolution limits (Å)	1.36	1.43	1.38
Unique reflections	10231	8595	9923
Completeness (%)	99.0	98.2	99.3
$R(I)_{merge}$ overall (at highest res., %)	2.9 (13.9)	3.0 (13.2)	3.8 (12.5)
$I/\sigma(I)$ overall (at highest res.)	17.1 (1.9)	15.7 (1.4)	17.7 (2.5)
R-value for all reflections (R_{free})	18.0 (18.9)	19.4 (21.3)	18.3 (20.0)
No. of residues	54	54	54
No. of protein atoms (inc. hydrogen)	419 (787)	419 (787)	419 (787)
No. of solvent waters (sulfate)	37 (1)	46	48
B_{mean} factor overall (waters only)	9.8 (22.4)	9.6 (22.1)	9.1 (20.9)
R.m.s. deviations from ideality			
Bond (Å)	0.021	0.021	0.022
Angle (°)	2.70	2.55	2.51

with clear tetrapod-shaped electron density in the oxidized crystal, but not in both forms of the reduced ones. Hydrogen atoms for the protein molecules were built with standard bond lengths and angles based on the positions of the non-hydrogen antecedents, and the corresponding positions were refined in the final stages of the refinements.

The *R*-factors for the final models for three Rds are from 18.0 to 19.4% (Table 1). The root-mean-square deviations (from standard geometry) of the three Rds are 0.021 Å for bonds and 2.59° for angles (averages for the three Rds). The coordinates of the Rd structures have been deposited in the Protein Data Bank (1SMM for the oxidized form, 1SMU for the drop-reduced form, and 1SMW for the soaked form).

Results

Reduction potential upon L41A mutation

A cyclic voltammogram of L41A Cp Rd is shown in Fig. 2. The reduction potential was determined to be 50 mV more positive than wild-type Cp Rd.

Crystallization of oxidized and reduced L41A Cp Rd

Oxidized crystals were obtained under normal atmospheric conditions (~20% oxygen). The colorless reduced crystals were obtained under two sets of conditions. In the first method, sodium dithionite as a reducing agent was added to both the reservoir and the crystal drop (drop-reduced). It was crucial to use the appropriate amount of reducing agent and to maintain the nitrogen atmosphere in the crystallization apparatus throughout the experiment. The protein reoxidized within 1–2 h if insufficient reducing agent was used or if there were trace amounts of oxygen in the crystallization chamber. In addition, the protein precipitated if too much sodium dithionite was used.

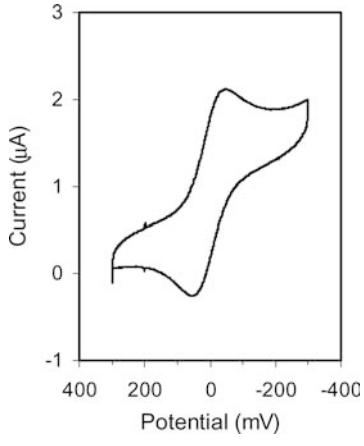

Fig. 2 Cyclic voltammograms of [L41A] Cp Rd in 0.1 M NaCl and 50 mM phosphate buffer at pH 7.6, with scan rate of 4 mV/s

In the second method, reduced crystals were directly prepared by dipping them into a cryo-solution containing sodium dithionite just before data collection (soaked). Reduction of the crystal was confirmed by monitoring the color of the crystal changing from deep red to colorless transparent as the reducing agent soaked into the crystal. Some crystals were fractured and/or melted during the soaking, as if there might be some structural rearrangement inside the crystalline lattice. However, by adjusting the concentration of sodium dithionite in the cryo-solution, some crystals survived the reduction process and, once reduced, the colorless state did not change throughout the whole data collection procedure.

Structural differences between oxidized and reduced forms of L41A Cp Rd

Though the volumes of the unit cells for the reduced Rds are slightly bigger than that for the oxidized form, the difference is small (0.4%). The overall conformations of the two oxidation states are very similar to wild-type Cp Rd, with average r.m.s. distances of 0.72(8) Å (all atoms except for the isopropyl group of residue 41), and to other Cp-type Rds [10, 16].

The geometry around the [Fe-S] redox center is changed slightly upon reduction. The four Fe–S distances of the reduced form are slightly longer (Fe–S elongation; +0.012 Å on average) than those of the oxidized form, whereas the six hydrogen bonds between the Sγ of the cysteines and nearby peptide amide nitrogens are shorter (S–N shrinkage; −0.064 Å on average) than the oxidized form (Fig. 3). Although the magnitude of this observed rearrangement upon reduction is small, it is a general trend in Rds. Similar rearrangements were observed in native Cp Rd (1FHH-1FHM pair; Fe–S elongation 0.096 Å, S–N shrinkage −0.042 Å), as well as in *Pyrococcus furiosus* Rd (1CAA-1CAD pair; Fe–S elongation 0.033 Å, S–N shrinkage −0.094 Å), where both of the oxidized and reduced structures are available at the protein data bank. Interestingly, elongation of the inner-shell Fe–S bonds are compensated by the shrinkage of outer-shell hydrogen bonds; consequently the overall positions of the backbone atoms around the [Fe-S] redox center remain unchanged upon the change in oxidation state.

The C-terminal amino acids, residues 53 and 54, are flexible, as reflected in both their high-temperature factors (*B*-factor, 27.1 on average) and the positional differences between the two oxidation states.

Unique water hydrogen-bonded to Cys9-Sγ in the reduced form of [L41A] Cp Rd

The removal of the isopropyl group at position 41 (i.e. substitution of leucine with alanine) does not perturb the local structure of [L41A] Cp Rd. The structure of the

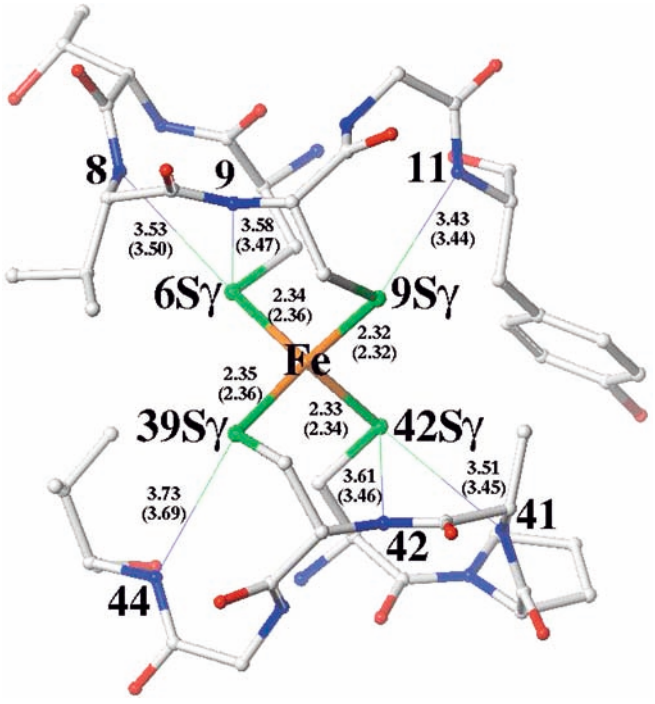

Fig. 3 The distances between Fe and Sγ, and between Sγ and amide N (Å), around the redox center of [L41A] Cp Rd. The values for the oxidized crystal are shown, and those for the reduced one (drop) are designated inside the parentheses

oxidized and reduced forms of [L41A] Cp Rd are very similar, with r.m.s. distances between the oxidized and drop-reduced forms of 0.67 Å, between the oxidized and soaked forms of 0.64 Å, and between the drop-reduced and soaked forms of 0.51 Å for all atoms, excluding the two flexible terminal residues.

The reduced form of [L41A] Cp Rd (both the drop-reduced and soaked crystals) has an unique water molecule hydrogen-bonded to Sγ-Cys9. Figure 4 shows the well-localized electron density (*B*-factors: 18.5 for drop-reduced and 21.9 for soaked) of this water molecule residing close to Sγ-Cys9 (3.37 Å) and Cβ-Ala41 (3.28 Å). In contrast, the oxidized form of [L41A] Cp Rd does not have a water molecule at this position, and it was not possible to find a reasonable electron density within the hydrogen bonding distance from Sγ atoms in oxidized Rd. This water molecule of the reduced Rds was also found at the same position in our previous report of the reduced wild-type Cp Rd crystal.

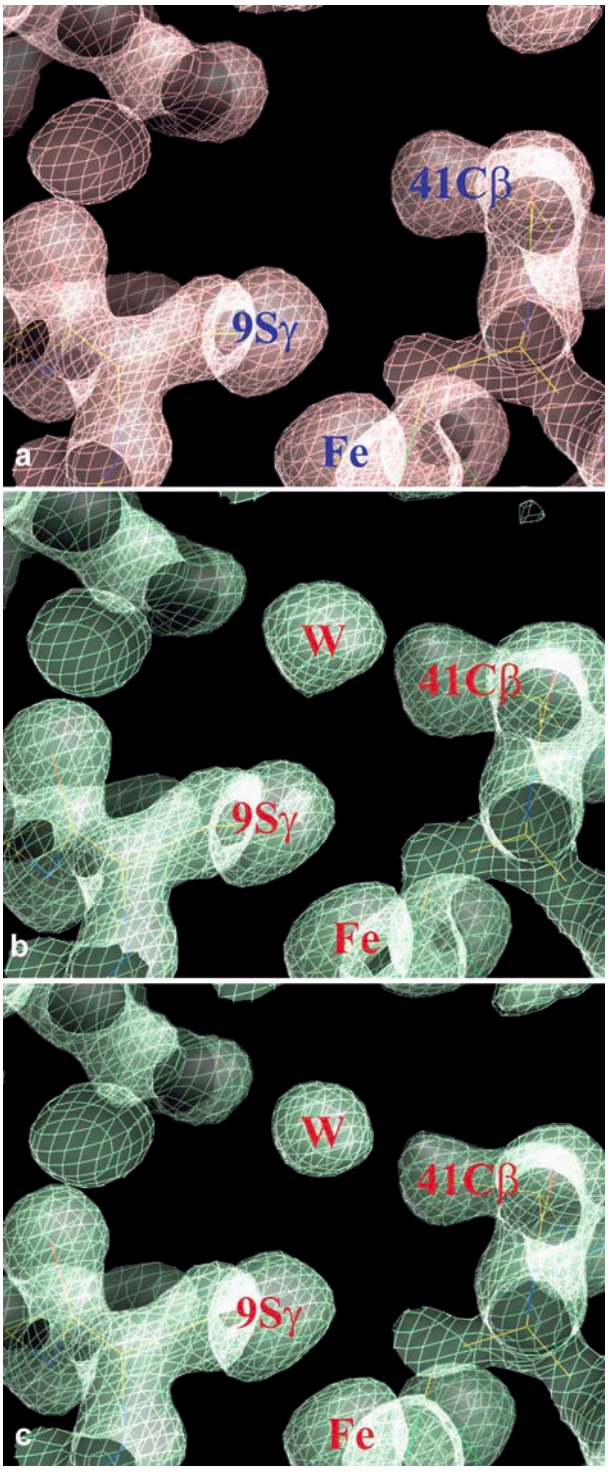

Fig. 4a–c The $2F_o-F_c$ electron density at the 1.0σ level in the vicinity of the Sγ atom of Cys9. (**a**) Oxidized form. (**b**) Reduced form (drop reduced). (**c**) Reduced form (soaked). Electron density corresponding to the hydrogen-bonded water is clear in the reduced forms (designated as W), while there is no electron density at this position in the oxidized form (**a**)

Discussion

Water molecule and electrochemistry

Both the reduced forms of [L41A] Cp Rd and wild-type Cp Rd (1FHM) contain a hydrogen-bonded water molecule to Sγ of Cys9. In contrast, the oxidized form of neither [L41A] Cp Rd nor wild-type Cp Rd (1FHH) has this specific hydrogen-bonded water, even though there is no steric hindrance that prevents a water molecule from hydrogen bonding at this position in the oxidized form of [L41A] Cp Rd. The electronic rearrangement around the iron center and/or the enrichment of negative charge in the Sγ of Cys9 upon reduction may induce

some electrostatic attraction towards the partial positive charge of hydrogen in the bound water molecule. We previously proposed [10] that this hydrogen bonding mechanism of the Sγ atom to the solvent water molecules stabilizes the reduced state and is gated by the side chain of leucine at position 41. This nonpolar side chain allows transient penetration of water molecules when it is in the reduced state [10]. The reduced state of the redox center is further stabilized by reducing the size of the side chain at position 41 and consequently allowing an easier entry of water molecules.

Iron-sulfur cluster

Upon reduction of Fe(III) to Fe(II), the attraction of Sγ electrons to the positive iron center decreases, resulting in an expansion of the iron-sulfur cluster. However, this expansion, or coordination energy change, is effectively compensated by the contraction of hydrogen bonds between Sγ and the backbone amide nitrogens, thus keeping the overall environment of the [Fe-S] redox center unchanged over the Fe(II)/Fe(III) transition. The increased attraction between the electron-enriched Sγ and amide hydrogen of the reduced state and the overall peptide backbone around the [Fe-S] center play an important role in keeping the redox center from expanding upon reduction.

This limited expansion observed in the [Fe-S] cluster is closely related to the relatively small energy difference associated with a change in oxidation state in Rds. The smaller inner-sphere reorganization energy associated with Fe(II)/Fe(III) couples of Rds, as compared to an inorganic $[FeCl_4]^{2-/-}$ cluster [17], are important for efficient electron transfer reactions in biological systems. The structural relaxation of the [Fe-S] center associated with a change in oxidation state is typical in Rds whose high-resolution structures of both redox states are available [10, 18].

Electron transfer pathway

Electron transfer could happen through either direct tunneling between proteins or a solvent-mediated tunneling. Based on the Cp Rd crystal structures of both oxidation states, we have previously proposed [10] that the electron transfer in Rds proceeds via a solvent-mediated process using the surface cysteines of Cys9 and Cys42.

Recently, Tezcan et al. [19] suggested that van der Waals interactions and water-mediated hydrogen bonds are effective coupling elements for electron tunneling across a protein–protein interface. Based on our observations of the water molecule directly hydrogen bonded to the cysteinate in the reduced state and the increase of the reduction potential of the [L41A] Cp Rd variant, it appears that the transfer of electrons is most likely a solvent-mediated process following the Fe(II)–Sγ(Cys9)–water–acceptor route. The umbrella of Val8 and Val44 residues over Cys42 makes the electron pathway more accessible through the Sγ atom of Cys9. The Sγ atom of Cys9 is exposed to the solvent by the ''flip-flop'' movement of the Leu41 side chain. This motion might serve as an automatic gate for the electron donor–acceptor protein during electron transfer.

If the reaction is a direct tunneling process (i.e. not a solvent-mediated one), the electron-acceptor atom of the acceptor molecule approaches directly to this position via a gate-like movement of the side chain in position 41 during the reaction. It is also plausible that Leu41 acts as an automatic gating mechanism for electrons to be transduced through a Fe(II)–Sγ(Cys42)–acceptor protein route.

In summary, the environment around the Sγ atom of Cys9 is an important determinant of electron transfer reactivity. The site provides a facilitated mechanism for the electron transfer reaction that is influenced by the side chain at position 41. The electron can be transferred through the sulfur atom via a solvent-mediated manner or directly to the electron acceptor molecule, and interaction with the solvent is an important determinant for the reduction potential of the redox site.

Acknowledgement This work was supported by grants from NIH to TI (R01-GM4503) and CHK (R01-GM66173).

References

1. Cammack R (1992) Adv Inorg Chem 38:281–322
2. Beinert H, Holm RH, Munck E (1997) Science 277:653–659
3. Sieker LC, Stenkamp RE, LeGall J (1994) In: Peck HD Jr, LeGall J (eds) Methods in enzymology, vol 243. Academic Press, San Diego, pp 203–216
4. Gray HB, Winkler JR (1996) Annu Rev Biochem 65:537–561
5. Swartz PD, Beck BW, Ichiye T (1996) Biophys J 71:2958–2969
6. Johnson MK (1998) Curr Opin Chem Biol 2:173–181
7. Meyer J, Moulis J-M (2001) In: Messerschmidt A, Huber R, Wieghardt K, Poulos T (eds) Handbook of metalloproteins, vol 1. Wiley, New York, pp 505–517
8. Maher MJ, Xiao Z, Wilce MC, Guss JM, Wedd AG (1999) Acta Crystallogr Sect D 55:962–968
9. Yelle RB, Park N-S, Ichiye T (1995) Proteins 22:154–167
10. Min T, Ergenacan C, Eidness M, Ichiye T, Kang C (2001) Protein Sci 10:613–621
11. Ausubel FM, Brent R, Kingston RE, Moore DD, Seidman JG, Smith JA, Struhl K (2000) Current protocols in molecular biology. Wiley, New York
12. Eidsness MK, Burden AE, Rchie KA, Kurtz DM Jr, Scott RA, Smith ET, Ichiye T, Beard B, Min T, Kang C (1999) Biochemistry 38:14803–14809
13. Smith ET, Bennett DW, Feinberg BA (1991) Anal Chim Acta 251:27–33
14. Navaza J (1994) Acta Crystallogr Sect A 50:157–163
15. Brunger AT (1992) X-PLOR: a system for crystallography and NMR, version 3.1. Yale University, New Haven
16. Dauter Z, Wilson KS, Sieker LC, Moulis JM, Meyer J (1996) Proc Natl Acad Sci USA 93:8836–8840
17. Kennepohl P, Solomon EI (2003) Inorg Chem 42:696–708
18. Day MW, Hsu BT, Joshua TL, Park JB, Zhou ZH, Adams MW, Rees DC (1992) Protein Sci 1:1494–1507
19. Tezcan FA, Crane BR, Winkler JR, Gray HB (2001) Proc Natl Acad Sci USA 98:5002–5006